

RECEIVED

AUG 7 1978

DIRECTORS OFFICE

FERMILAB

400 GeV/c pp Elastic Scattering: Energy and Angle

Dependence at High Momentum Transfer

S. Conetti, C. Hojvat,^(a) D. G. Ryan, K. Shahbazian,

D. G. Stairs, and J. Trischuk

McGill University, Montreal, Quebec H3A 2T8, Canada

and

W. Faissler, M. Gettner, J. R. Johnson,^(b) T. Kephart,E. Pothier, D. Potter,^(c) and M. Tautz

Northeastern University, Boston, Massachusetts 02115

and

P. Baranov,^(d) J. L. Hartmann, J. Orear, S. Rusakov,^(d) and J. Vrieslander

Cornell University, Ithaca, New York 14853

Abstract

Proton-proton elastic scattering at 400 GeV/c has been measured in the region $5.4 < -t < 14.4 \text{ GeV}^2$ with no sign of a second dip or "break". If the data are fit by $\exp(At)$, the slope A decreases from 1.5 ± 0.1 to $0.7 \pm 0.2 \text{ GeV}^{-2}$ over the range. At fixed t the 400 GeV/c cross sections are about 0.6 times those at 200 GeV/c in this t -range. At fixed $\theta_{\text{cm}} = 15^\circ$, $d\sigma/dt \propto s^{-n}$ where $n = 9.7 \pm 0.3$.

Results from the CERN ISR⁽¹⁾ show that $d\sigma/dt$ is essentially independent of s in the region $500 < s < 3800 \text{ GeV}^2$ up to $-t = 3.6 \text{ GeV}^2$. (The only s -dependence is a small shift in position of the $-t = 1.4 \text{ GeV}^2$ dip.) This raises the question whether asymptopia has been reached for all values of t when $s > 500 \text{ GeV}^2$ (a fixed target beam momentum of $280 \text{ GeV}/c$). Results of this experiment show that for $-t > 5 \text{ GeV}^2$ there is still a significant energy dependence, but that it is decreasing with increasing s . In addition there is no evidence for a predicted second dip⁽²⁾ or for a slope of $d\sigma/dt$ consistent with diffraction scattering.⁽³⁾

The experiment was performed in the Proton West Area of the Fermi National Accelerator Laboratory using the same apparatus shown in Figure 1 of the previous letter reporting our $20 \text{ GeV}/c$ results.⁽⁴⁾ The only significant difference was the use of a third analysing magnet in the forward spectrometer. The acceptances and resolutions were comparable in both experiments, and most of the normalization errors cancel when taking the ratio of the 200 to $400 \text{ GeV}/c$ cross sections. Typical beam intensities were $\sim 5 \times 10^{11}$ protons per pulse with a spot size of $\pm 1.9 \text{ mm rms}$ and beam divergence of $\pm 6 \times 10^{-5}$ radians at the target. The limitation on beam intensity was due to accidental triggers which were not allowed to exceed 30 per pulse. At $400 \text{ GeV}/c$ three different settings of the forward spectrometer and target position were necessary in order to cover the entire t -range. The low- t run covered $5.4 < -t < 9.2 \text{ GeV}^2$, the mid- t run covered $8.4 < -t < 12.8 \text{ GeV}^2$, and the high- t run covered $10.0 < -t < 14.4 \text{ GeV}^2$. The $200 \text{ GeV}/c$ running took place between the mid- t and high- t runs. All running took place in one uninterrupted block of time. Results from the 3 individual $400 \text{ GeV}/c$

runs are shown in Fig. 1 plotted against p_t . Since the absolute cross sections in the regions of overlap agree within errors, the overlapping cross sections have been combined statistically and are shown in Fig. 2 where $d\sigma/dt$ is shown as a function of t together with other results from 19.3 GeV/c,⁽⁵⁾ 21.3 GeV/c,⁽⁶⁾ and 28 GeV/c.⁽⁷⁾

We use Fig. 3 to illustrate the low level of inelastic background at even the highest t . Fig. 3a shows those events in the high- t run which have at least one track in each spectrometer arm which can be tracked back to the target. No other cuts have been made. The dashed line shows a possible interpolation of inelastic events under the elastic peak leading to an estimate of $\sim 60\%$ background before making the remaining cuts. Fig. 3b shows that when coplanarity, $(t_{\text{forward}} - t_{\text{recoil}})$, opening angle, and recoil missing mass cuts are made, the inelastic background drops down to $(4 \pm 1)\%$. (More details on the cuts and the experimental setup are given in Reference 4.) Inelastic background in the mid- t run was $(6 \pm 2)\%$. In the low- t run the scattering angles were too small to allow room for proper collimation between the beam and scattered protons. Because of this the inelastic background rose to $(12 \pm 2)\%$ for the low- t run. Fig. 3a also shows that in the worst case $\sim 3\%$ of the triggers which contained tracks originating in the target were elastics.

The efficiencies of all MWPC's were continuously monitored and averaged about 94% per plane. The resulting probability that our system miss either the forward or recoil track was 12%. Cross sections were corrected for this 12% loss and an additional 17% loss due to particle absorption in the air path and detectors. Reconstruction loss was about 2%. Loss due to elastic cuts was $(5 \pm 2)\%$. Beam monitoring was the same as in

Reference 4 with an overall 20% (rms) normalization uncertainty. This uncertainty is reduced to $\sim 5\%$ when taking ratios of the 200 to 400 GeV/c cross sections. The rms spread of the t -determination is about $\pm 0.34 \text{ GeV}^2$ at $-t = 5 \text{ GeV}^2$; it decreases linearly to about $\pm 0.15 \text{ GeV}^2$ at $-t = 7 \text{ GeV}^2$; and then increases linearly to $\pm 0.19 \text{ GeV}^2$ at $-t = 14 \text{ GeV}^2$. The absolute calibration of t is accurate to within one binwidth. This uncertainty is due mainly to a $\pm 1\%$ variation in the momentum of the primary beam. A shift in the t -scale of one binwidth could cause a maximum change of $d\sigma/dt$ of $\sim 20\%$.

The initial slope $d(\ln d\sigma/dt)/dt$ of our 400 GeV/c results is found to be $1.5 \pm 0.1 \text{ GeV}^{-2}$ at $-t = 6 \text{ GeV}^2$ and it gradually drops to $0.7 \pm 0.2 \text{ GeV}^{-2}$ at $-t \approx 12 \text{ GeV}^2$. As seen in Fig. 1 much of this change in slope is removed if the data are plotted vs. p_t . Then the best fit is $d\sigma/dt = 3.2 \times 10^{-28} \exp(-6.2 p_t) \text{ cm}^2/\text{GeV}^2$.

Fig. 2 shows that $d\sigma/dt$ at fixed t is still dropping with energy. At all values of t shown, the ratio of $d\sigma/dt$ at 400 GeV/c to 200 GeV/c is about 0.6 ± 0.2 . At any fixed value of t , $d\sigma/dt$ drops with energy, but the rate of drop decreases rapidly with beam momentum. The power law dependence of this decrease is given by the slopes of the curves in Fig. 4 where $\log(d\sigma/dt)$ is plotted vs. $\log p_{\text{lab}}$. We see that at $-t = 3.6 \text{ GeV}^2$, $d\sigma/dt$ becomes energy independent above $\sim 200 \text{ GeV}/c$. At $-t = 6 \text{ GeV}^2$ asymptopia is not quite reached in our energy region. At higher $|t|$ it appears that one must go to increasingly higher energies in order to achieve energy independence.

The s-dependence of $d\sigma/dt$ at constant center-of-mass angle θ can be obtained from our results. For fixed θ , our 200 and 400 GeV/c results overlap only in the region 13° and 15° where we find $n = 9.1 \pm 0.3$ at 13° and $9.7 \pm .3$ at 15° for the form $[d\sigma/dt]_{\theta=\text{constant}} \propto s^{-n}$. At 15° this is in agreement with the constituent interchange model which predicts $n = 10$.⁽⁹⁾ Whether $n = 10$ would work for larger angles at this energy is not known.

We wish to thank B. Cox, T. Murphy, J. Peoples, R. Rubinstein, R. Schaeren, and the Proton Laboratory staff for their help and cooperation. This work was supported in part by the U. S. National Science Foundation, the National Research Council of Canada through the Institute of Particle Physics, and the Ministry of Education of Quebec.

References

- (a) Present address: Fermilab, Batavia, IL 60510.
 - (b) Present address: University of Wisconsin, Madison, Wisc. 53706.
 - (c) Present address: Rutgers University, New Brunswick, NJ 08903.
 - (d) Permanent address: Lebedev Physical Institute, Moscow, U.S.S.R.
1. N. Kwak, et al., Phys. Lett. 58 B, 233 (1975).
 2. T. T. Chou and C. N. Yang, Phys. Rev. D. 17, 1889 (1978).
 3. U. P. Sukhatme, Phys. Rev. Lett. 38, 124 (1977).
 4. J. L. Hartmann, et al., Phys. Rev. Lett. 39, 975 (1977).
 5. J. V. Allaby et al., Phys. Lett. 25B, 156 (1967).
 6. J. V. Allaby et al., Nucl. Phys. B52, 316 (1973).
 7. G. Cocconi et al., Phys. Rev. 138B, 164 (1965).

8. H. De Kerret et al., Phys. Lett. 62B, 363 (1976).
9. D. Sivers, S. J. Brodsky, and R. Blankenbecler, Phys. Rep. 23C, 1 (1976).

FIGURE CAPTIONS

Fig. 1. 400 GeV/c results for the three geometries of this experiment are plotted vs. p_t .

Fig. 2. Combined results of our 400 GeV/c experiments are plotted vs. t along with our 201 GeV/c results⁽⁴⁾ and results of other experiments.^(5,6,7,8) the curves are drawn to guide the eye.

Fig. 3. Number of elastic candidates from our highest- t run plotted vs. P_f , the momentum as measured by the forward spectrometer. The momentum-transfer range is $10.0 < -t < 14.4 \text{ GeV}^2$. (a) All events where there is at least one track in each arm appearing to originate from the target. (b) Same conditions as in (a) except that all elastic cuts have been made except P_f . The dashed line shows our estimate of the inelastic background under the elastic peak.

Fig. 4. $d\sigma/dt$ vs. P_{beam} for $-t = 3.6, 6, 8, 10, \text{ and } 12 \text{ GeV}^2$. Some of the points shown are interpolations from nearby experimental points. The curves are drawn to guide the eye.

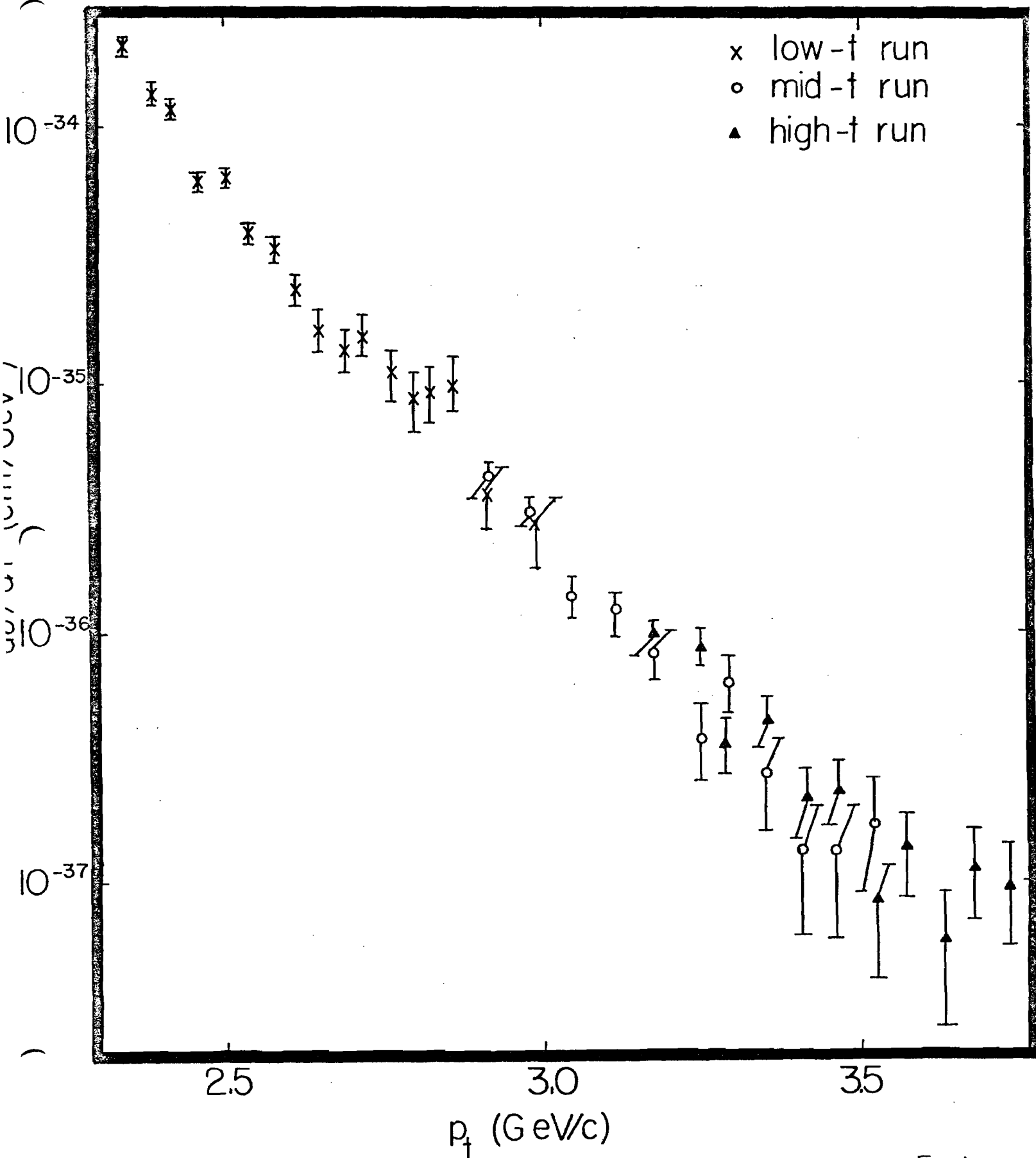
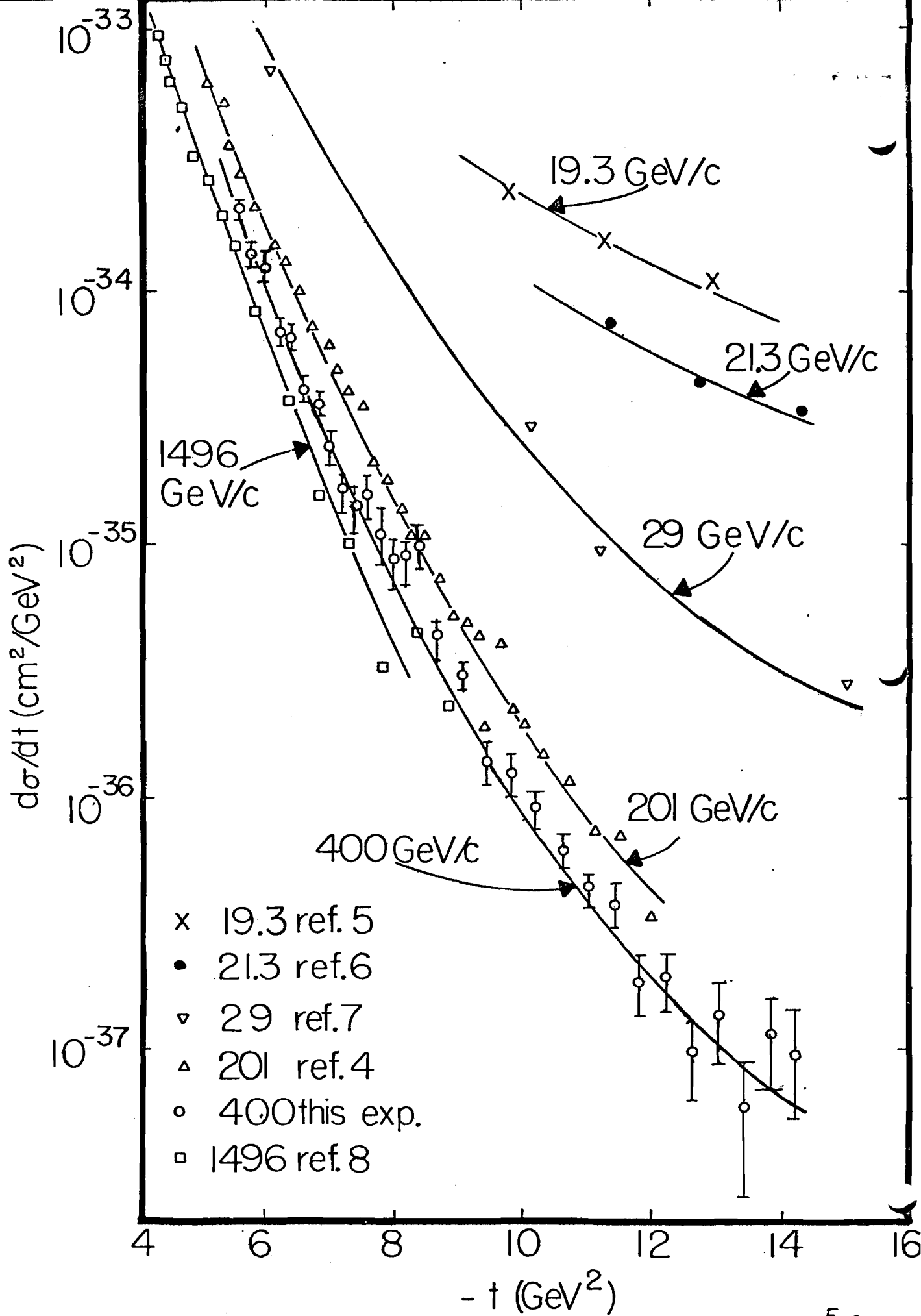


Fig. 1



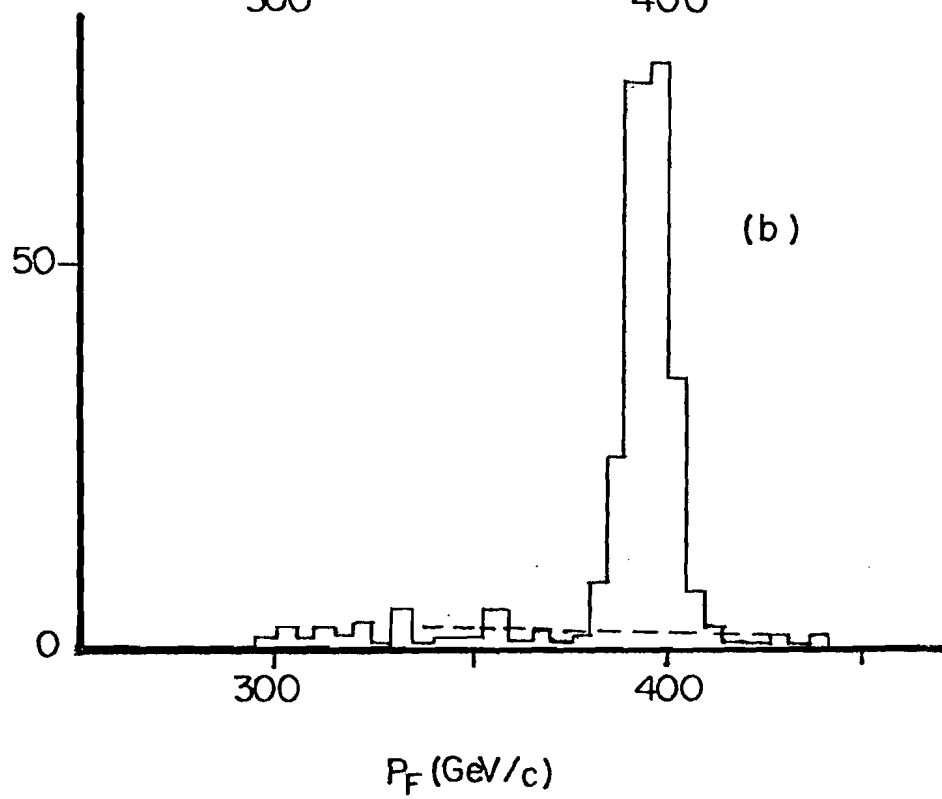
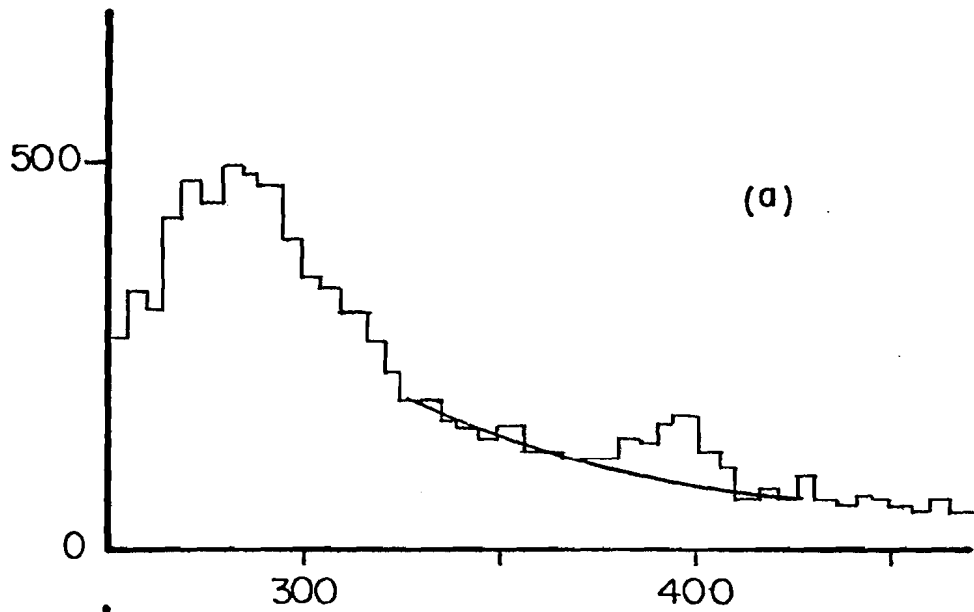


Fig 3

0850778

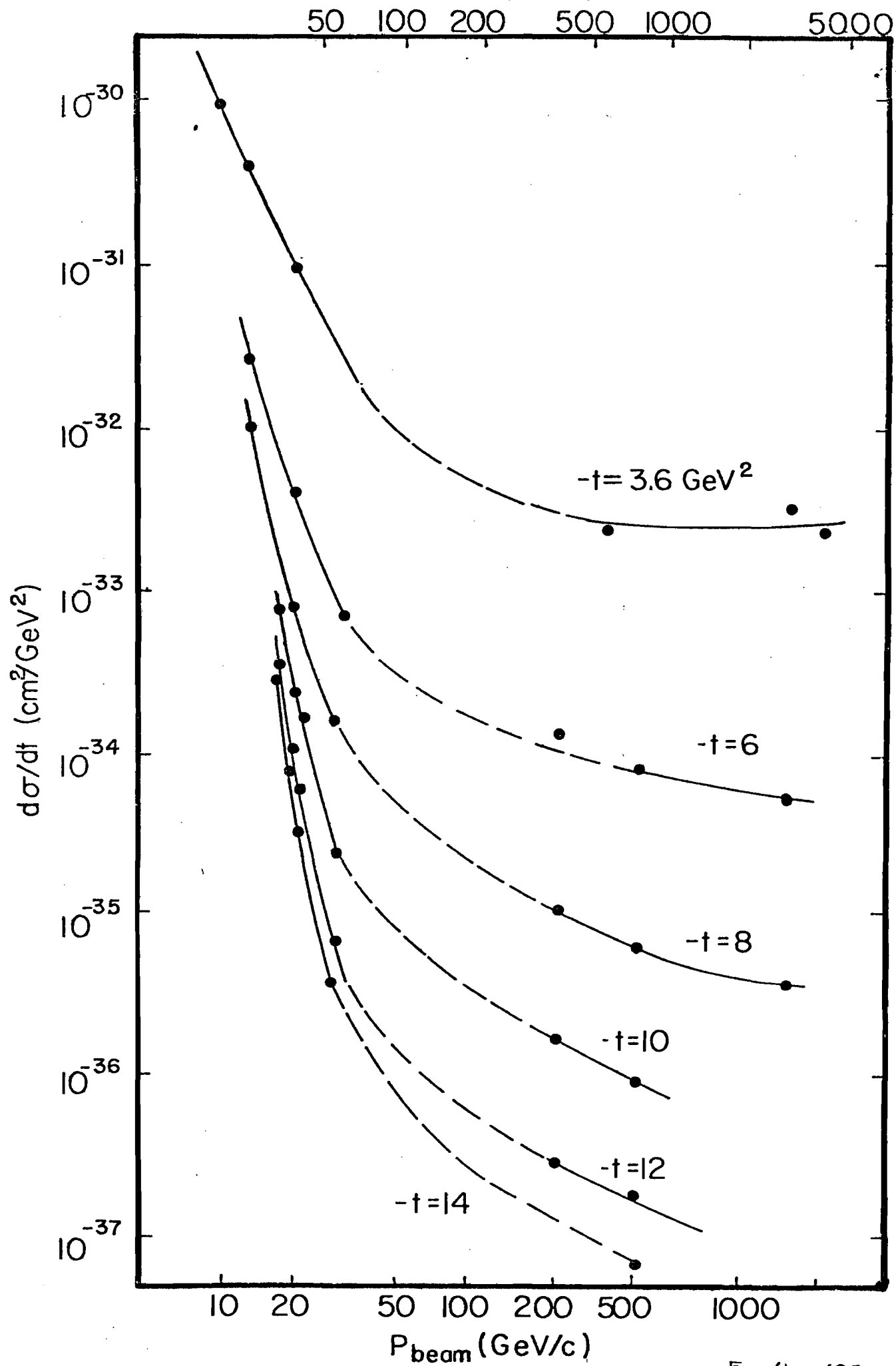


Fig. 4 1850779